M-AM-Sym I-1

CALCIUM BINDING TO PROTEINS: A STRUCTURAL PERSPECTIVE. N.C.J. Strynadka and M.N.G. James, Medical Research Council of Canada Group in Protein Structure and Function, Department of Biochemistry, University of Alberta, Edmonton, Alberta, Canada T6G 2H7

Analysis of the calcium binding site architecture in a number of high resolution crystallographic protein structures indicates several commonalities.[1,2] The majority of sites are situated in loop conformations on the surface of the protein. Each site generally contributes seven oxygen ligands to the metal ion. The oxygen atoms (from carboxylates, amides, mainchain carbonyl and water molecules) are arranged at the vertices of a pentagonal bipyramid with the average Ca^{2+} ion to oxygen ligand distance ~ 2.4 Å (regardless of ligand type). Unlike the phosphate binding proteins, helix dipoles do not play a direct role in calcium binding. Hydrogen bonding of the calcium ligands is extensive and is supported by a shell of polar and charged amino acids surrounding the calcium binding site. The extensive use of hydrogen bonding serves not only to orient the side and main chain conformations required for effective ion binding but also to stabilize the repulsive electrostatic forces associated with the close proximity of negatively charged oxygen atoms in the calcium coordination sphere.

The binding of calcium to a particular protein mediate a variety of biological functions. These include stabilization of tertiary structure to protect against proteolytic degradation, enhancement of enzymatic catalysis and induction of conformational movements to facilitate interaction with target molecules. A molecular model describing a Ca^{2+}-induced conformational change in the intracellular proteins troponin C and calmodulin proposes the exposure of a hydrophobic pocket upon calcium uptake. These hydrophobic regions can readily accommodate the molecular structure of several known antagonists of troponin C and calmodulin activity, including the antipsychotic trifluoperazine and the family of amphiphilic, helical peptides known as the mastoporans.[3,4]

[1] Strynadka, N.C.J. and James, M.N.G. (1989). *Ann. Rev. Biochem.* 58:951-958.

[2] McPhalen, C., Strynadka, N.C.J. and James, M.N.G. *Adv. Protein Chem.* (in press).

[3] Strynadka, N.C.J. and James, M.N.G. (1988). *Proteins: Structure, Function and Genetics* 3:1-17.

[4] Strynadka, N.C.J. and James, M.N.G. (1990) *Proteins: Structure, Function and Genetics* 7:234-248.

M-AM-Sym I-2

THE ROLE OF CALCIUM IN INTERFACIAL CATALYSIS: THE MECHANISM OF PHOSPHOLIPASE A2. Paul B. Sigler, Dept. of Molecular Biophysics and Biochemistry, Howard Hughes Medical Institute, Yale Univ., New Haven, CT, 06511.

A chemical description of the calcium-dependent action of phospholipase A2 (PLA2) can now be inferred with confidence from three high resolution X-ray crystal structures. The first is the structure of PLA2 from the venom of the Chinese cobra (*Naja naja atra*) in a complex with a phosphonate transition-state analogue. This enzyme is typical of a large, well studied homologous family of PLA2s. The second is a similar complex with the evolutionary distant bee-venom PLA2. The third structure is the uninhibited PLA2 from Chinese cobra venom. Despite the different molecular architectures of the cobra and bee-venom PLA2s, the transition-state analogue interacts in a nearly identical way with the catalytic machinery of both enzymes. The Ca^{2+} cofactor is septa-coordinated with oxygen atoms in pentagonal bipyramidal geometry. Two of the seven sites in the uninhibited enzyme are water molecules which are replaced during catalysis by oxygen atoms of the transition state including the oxyanion of the tetrahedral intermediate.

The disposition of the fatty acid side chains suggests a common access route of the substrate from its position in the lipid aggregate to its productive interaction with the active site. Comparison of the cobra-venom complex with the uninhibited enzyme indicates that optimal binding and catalysis at the lipid/water interface is due to facilitated substrate diffusion from the interfacial binding surface to the catalytic site rather than one allosteric change in the enzyme's conformation. There is an important change in structure, however; a second bound calcium ion changes its position upon the binding of the transition-state analogue, suggesting a mechanism for augmenting the critical electrophile.

M-AM-Sym I-3

A MULTI-DIMENSIONAL NMR STUDY OF CALMODULIN AND ITS COMPLEX WITH A MYOSIN LIGHT CHAIN KINASE FRAGMENT. **Mitsuhiko Ikura, Gaetano Barbato, Marius Clore, Angela Gronenborn, Lewis Kay, Silvia Spera, Guang Zhu, and Ad Bax. Laboratory of Chemical Physics, NIDDK, NIH, Bethesda, Maryland 20892.**

New heteronuclear triple resonance [^{1}H,^{13}C,^{15}N] 3D NMR techniques, recently developed in our laboratory, have permitted us to make complete backbone and side chain assignments for Ca^{2+}-loaded calmodulin in the absence and presence of the myosin light chain kinase 26-residue peptide fragment, M13. The new methodology relies on heteronuclear J couplings in the $^{15}N/^{13}C$ enriched protein to obtain resonance assignment information, and to resolve the NOESY spectrum into higher dimensionality. Using this approach we have completed determination of the secondary structure of calmodulin in the absence and presence of M13. In the absence of M13, the solution conformation is quite similar to the X-ray crystal structure, with the exception of residues 78-84 in the central helix region. The solution structure includes a tightly bound water molecule in this region, that causes the helix to bent and stabilizes the "bent" form of the helix. In the presence of M13, substantial changes in ^{1}H, ^{15}N and ^{13}C chemical shifts of the backbone atoms occur throughout the protein, although these changes are most distinct in the central helix, the C-termianl helix E_I, and the N-terminal helix F_{IV}. Preliminary NOE analysis indicates that all secondary structural elements, observed in the absence of M13, are preserved in the complex. However, significant changes in secondary structure are observed in residues 74-77.

M-AM-Sym I-4

CALCIUM PUMPS AND CHANNELS IN THE SARCOPLASMIC RETICULUM David H. MacLennan, Banting & Best Dept. of Med. Res., University of Toronto, Toronto, Ont., Canada. M5G 1L6

The sarcoplasmic reticulum regulates the concentration of Ca^{2+} ions within muscle cells through a Ca^{2+} pump, (Ca^{2+} ATPase) and a Ca^{2+} release channel (ryanodine receptor), thereby regulating muscle contraction. We have cloned cDNAs encoding Ca^{2+} ATPases and ryanodine receptors from both skeletal and cardiac muscles and, on the basis of their amino acid sequences inferred from their cDNAs, have made deductions concerning their secondary structures and active sites. These deductions have led us to test models for Ca^{2+} transport and release through expression of the proteins in functional form, mutagenesis and measurement of altered functions. Mutation of about 250 of the 1000 amino acids making up the Ca^{2+} pump from fast-twitch skeletal muscle has indicated that the sites of high affinity Ca^{2+} binding are located in the center of the transmembrane domain and are made up from residues located in transmembrane sequences M4, M5, M6 and M8. The ATP binding site appears to be located in the headpiece and is made up from a series of loop sequences connecting alternating alpha helices and beta strands. In our present model, Ca^{2+} transport occurs through binding to high affinity sites accessible to the cytoplasm in the E1 conformation, followed by release to the lumen from low affinity sites which form during the ATP-induced transition of the protein from the E1 to the E2 conformation.

Cloning of cDNA encoding the ryanodine receptor has led to the prediction that up to 5% of its 5000 amino acids might exist in transmembrane sequences near the COOH-terminal end of the protein, while the remainder are cytoplasmic, making up the foot structures connecting the sarcoplasmic reticulum and the transverse tubule. We have localized the gene for this protein to human chromosome 19q13.1 and have shown linkage between the RYR1 gene and the gene responsible for the predisposition to malignant hyperthermia (MH). Detection of mutations in the RYR1 gene, leading to MH, should provide insight into the regulatory region of the Ca^{2+} release channel.

(Supported by grants from the MRC, NIH, MDAC and HSFO)

M-AM-A1

MUTATIONS ALTERING IONIC SELECTIVITY OF THE SHAKER K^+ CHANNEL. Andrea Yool, Irene Inman and Thomas Schwarz (intro. by T.Ryan); Dept. Molec.& Cell. Physiol., Stanford University, CA 94305.

Site-directed mutagenesis of *Drosophila* ShakerB within a highly conserved region (H5, 429 to 455) has generated K^+ channels with increased ionic permeabilities to NH_4^+ and Rb^+, but not Na^+. Wildtype and mutant channels were expressed in *Xenopus* oocytes, and analyzed by two-electrode voltage clamp and patch clamp. Most conservative single amino acid substitutions did not produce detectable currents. Wildtype selectivity, determined from reversal potentials in biionic conditions with the test ion external and K^+ internal, followed the sequence $K^+ > Rb^+ > NH_4^+ >> Na^+$ (Fig.1). Two mutations (F433S and T441S) dramatically increased unit conductance to NH_4^+ and shifted the biionic reversal potential (NH_4^+ external, K^+ internal) by +40 mV (Fig. 2), giving a selectivity sequence of $NH_4^+ \sim K^+ \sim Rb^+ >> Na^+$; a more subtle mutation (F433Y) showed intermediate effects. Comparable effects were seen with Rb^+, though the reversal potential shifts were smaller. Reversal potentials in symmetrical K^+ were near 0 mV for wildtype and all mutant channels. McKinnon and Yellen (*Science*, in press) have shown that H5 is bounded on both sides by sites that tolerate non-conservative changes and influence TEA binding, defining the putative pore mouth. In our mutations within H5, blockade of macroscopic currents by external TEA is not altered. The positions of residues influencing permeation are consistent with a channel model in which H5 lines the inner pore. In general, our mutations do not alter activation or inactivation rates; however, the substitution T442S slows macroscopic inactivation about 10-fold with little effect on selectivity, suggesting this site may interact with other regions of the channel controlling kinetic properties. (Supported by grants NIH R01 GM42376 to TLS, and NIH R01-15963 to L. Jan.)

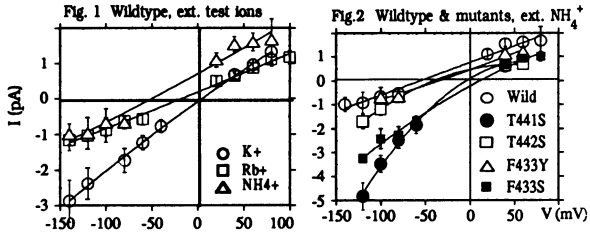

M-AM-A2

CHARACTERIZATION OF THE SHAW-LIKE CLASS OF K^+ CHANNEL GENES IN MAMMALS. Sen, K., Vega-Saenz de Miera, E., Chiu, N., Lin, J.W., Lau, D. and Rudy, B. Depts. of Physiology & Biophysics and Biochemistry, New York University Medical Center, N.Y. (Introduced by: Sylvia Lee-Huang)

We report the deduced amino acid sequence and electrophysiological properties of two novel K^+ channel genes in rat. Both genes RKShIIIC and RKShIIID shared a large amount (more than 70%) of amino acid identity with two previously reported genes (NGK2 and RKShIIIA). Amino acid sequence comparisons and phylogenetic analysis indicate that these genes are distantly related to the Shaw gene in Drosophila. RKShIIIA and NGK2 appear more more similar to each other, than to ShIIIC and ShIIID. RKShIIIA has a long insert in the amino end region of the protein. This insert contains strings of prolines and serines and might be a site of cytoplasmic O-glycosylation. The functional significance of this insert is, however, not known. An important difference between RKShIIIA or NGK2 and RKSIIIC or D is an amino acid substitution in H5, a region suggested to be involved in ionic selectivity. RKShIIIC and D contain a lysine in a position occupied by glutamine in RKShIIIA and NGK2. This amino acid is four positions (C-terminal) from an aspartic acid which is conserved in all Shaker family potassium channel genes, and may be located near the channel's mouth. The possible role of this substitution in regulation channel conductance will be discussed. The sequence of some of these genes will be compared to that of their homologues in humans. This comparison helps identify highly conserved amino acids which may be important for the functional characteristics of these genes. Supported by NIH Grant: GM26976 to BR.

M-AM-A3

MUTATIONS OF *SHAKER* K^+ CHANNELS THAT AFFECT BOTH OUTWARD CONDUCTANCE AND INACTIVATION E.Y. Isacoff, Y.N. Jan and L.Y. Jan. Howard Hughes Medical Institute and the Departments of Physiology and Biochemistry, University of California, San Francisco, CA 94143.

In an attempt to identify the region of the *Shaker* K^+ channel that forms the inner part of the pore we have made single amino acid substitutions in which negatively charged, acidic residues in proposed cytoplasmic domains of the channel were replaced by the uncharged amino acid glutamine. In this way we have found a single site, E395 (that is located in a proposed cytoplasmic loop between two putative transmembrane segments S4 and S5 and which is conserved among all the known potassium channels), at which neutralization reduced single channel outward currents to less than 25% of wild-type. This mutation also slowed macroscopic inactivation by more than 5 fold. Similar substitutions at several other conserved, putatively cytoplasmic glutamates outside the S4-S5 loop had no such effects. Conservative substitutions at several other conserved residues in the S4-S5 loop--L385, T388 and S392--had the same dual effect of reducing channel conductance and altering inactivation kinetics, whereas substitutions at poorly conserved residues in the loop had no such effects. Mutations at all four of the residues that affected conductance and inactivation had little or no effect on the voltage dependence of channel activation or on the strong dependence of channel equilibrium potential on external K^+. Based on our findings, and on the intervals at which conserved residues occur in the S4-S5 loop, we propose that the S4-S5 loop a) is located at or near the pore; b) interacts with the N and C termini of the protein to mediate inactivation gating; and c) may form an α-helix in which residues L385, T388, S392 and E395 lie on the same face of the helix.
(Supported by HHMI and by an MDA post-doctoral fellowship to E.Y.I.)

M-AM-A4

MOLECULAR SEPARATION OF TWO INACTIVATION PROCESSES IN *SHAKER* POTASSIUM CHANNELS. W. N. Zagotta, T. Hoshi, R. W. Aldrich. Department of Molecular and Cellular Physiology, Stanford University School of Medicine, Stanford, CA 94305.

Shaker potassium channels exhibit fast and slow components of inactivation. In the alternatively spliced variant ShB, the fast component of inactivation is mediated by the NH_2-terminus, a part of which functions as a "ball and chain". This fast component of inactivation is eliminated by many mutations of the NH_2-terminus (IR mutations). In IR mutants, macroscopic currents inactivate typically with a time constant of 1 to 2 s. This inactivation rate is enhanced and the recovery from inactivation is slowed when the COOH-terminal end of the IR mutant is replaced by that of the ShA variant. This suggests that inactivation controlled by the COOH-domain (C-inactivation) occurs by a process separate from that controlled by the NH_2-terminus (N-inactivation). The rate of C-inactivation in ShA is much faster than that of ShB-IR, and slower than but in the same range as that of ShB N-inactivation. As is the case with N-inactivation, C-inactivation is voltage independent in the range of 0 to +50 mV. Large deletions in the putative cytoplasmic region following S6 in both ShA and ShB variants had little effect on the rate of C-inactivation. Outside of the putative cytoplasmic domain, ShA and ShB differ only in 3 amino acid positions, 2 in S6 and 1 in the linker between S5 and S6. Of the three differences between ShA and ShB that exist outside of the putative cytoplasmic region, a single amino acid change at position 463 in S6 (alanine in ShB and valine in ShA) accounts for the differences in C-inactivation. Substituting this amino acid with other nonpolar amino acids produced graded effects on C-inactivation. In addition, some of these mutations altered the single-channel conductance. C-inactivation in *Shaker* potassium channels is in many ways similar to inactivation in delayed rectifier channels, suggesting that the same mechanisms may be involved.

M-AM-A5

DIFFERENT SITES FOR TETRAETHYLAMMONIUM BLOCKADE OF CLONED DELAYED RECTIFIER K^+ CHANNELS by [1]M. Taglialatela, [1]J.A. Drewe, [1]A.M.J. VanDongen, [1]R.H. Joho, [1]A.M. Brown and [2]G.E. Kirsch (Introduced by R.E. Anderson). [1]Department of Molecular Physiology and Biophysics and [2]Department of Anesthesiology, Baylor College of Medicine, 1 Baylor Plaza, 77030 Houston, TX.

Mammalian delayed rectifiers (DR) K^+ channels differ in their biophysical and pharmacological properties. These differences are likely to be due to the unique molecular architecture of each of these channels. In order to probe channel structure with the blocking ion tetraethylammonium (TEA), we have investigated the effects of external and internal application of TEA on whole cell currents in voltage-clamped *Xenopus* oocytes injected with the cRNA encoding for four cloned DR K^+ channels from the mammalian brain: DRK1, RCK1, RCK2 and NGK2. External TEA blocked RCK1 and NGK2 with high affinity (apparent K_d 0.2 mM), RCK2 with intermediate affinity (K_d 1.4 mM) and DRK1 with low affinity (K_d 5-10 mM). Internal application of TEA caused a comparable high affinity block (K_d 0.2 mM) of DRK1, RCK1 and RCK2, while NGK2 was at least 30 times less sensitive (K_d 4 mM). The external site appears to show no (in RCK1 and NGK2) or very small (in RCK2) voltage-dependence. By contrast, TEA K_d at the internal site, in DRK1, RCK1 and RCK2, decreases e-fold/150 mV depolarization. This voltage-dependence arises from the fact that the internal TEA binding site is within the membrane electric field, with an apparent valence (δ) of about 0.2. Furthermore, at variance with the squid axon DR, inward K^+ currents do not remove internal TEA block. However, in analogy to the reported effects on the squid axon, the lipophilic TEA derivative tetrapentylammonium (TPeA) blocked DRK1 and RCK2 channels more effectively than TEA, suggesting the existence of an hydrophobic region in the proximity of the TEA binding site. The definition of these biophysical properties characterizing the internal and external TEA block is a first step toward a better understanding of the structural parts of the channels involved in the formation of its external and internal mouth. (Supported by NIH NS 23877 and NS 28407).

M-AM-A6

MECHANISM OF TETRAETHYLAMMONIUM BLOCK IN CLONED RAT BRAIN K^+ CHANNELS. G. E. Kirsch[1,2], M. Taglialatela[2] and A. M. Brown[2]. [1]Department of Anesthesiology and [2]Department of Molecular Physiology and Biophysics. Baylor College of Medicine, Houston, TX 77030.

The effects of tetraethylammonium (TEA) and tetrapentylammonium (TPeA) ions on single, voltage-dependent delayed rectifier K^+ channels; RCK2, DRK1 and NGK2; expressed in *Xenopus* oocytes were determined in excised inside-out membrane patches. Cytoplasmic application of TEA to RCK2 and DRK1 caused decreased channel open time, increased number of openings/burst and increased intraburst closed interval. The effect of TEA on open times, but not on closed times was concentration-dependent. From these data ON and OFF rates for block of the open channel of 1.6 ms^{-1} mM^{-1} and 0.8 ms^{-1}, respectively, were obtained. The apparent K_d = 0.5 mM is similar to that obtained from block of whole cell currents. Depolarization potentiated the effect of TEA on open time (δ=0.25). The effect of cytoplasmic application of TPeA to RCK2 was similar to that of TEA, but TPeA was 200 times more potent. NGK2 was resistant to the effects of cytoplasmic TEA. Extracellular application of TEA to RCK2 caused an apparent reduction of single channel amplitude. The results suggest that TEA interacts with open channels and that the cytoplasmic mouth of either RCK2 or DRK1 is structurally different from that of NGK2 (supported by NIH HL-36930, NS-23877, and the American Heart Association-Texas Affiliate).

M-AM-A7

A SEQUENCE OF TWENTY-SIX AMINO ACIDS CONTROLS ION PERMEATION AND BLOCK IN A CHIMERIC K^+ CHANNEL

H.A. Hartmann, J.A. Drewe, G.E. Kirsch, M. Taglialatela, R.H. Joho and A.M. Brown. Departments of Molecular Physiology and Biophysics and Anesthesiology, Baylor College of Medicine, Houston, TX 77030.

Two types of K^+ channels, NGK2 and DRK1 differ in conductance and in the affinities with which TEA blocks external and internal sites. NGK2 has more than twice the conductance of DRK1 and is blocked best at an external site whereas DRK1 is blocked best at an internal site. The block at the internal site of DRK1 is voltage dependent. We have replaced a 26 amino acid sequence in DRK1 between transmembrane segments S5 and S6 with the corresponding sequence from NGK2. To accomplish this silent restriction sites were first introduced into DRK1 to flank the 26 amino acid sequence. The corresponding DNA sequence from NGK2 was synthesized by PCR with primers which included these same silent restriction sites. cRNA of the chimeric channel was transcribed and injected into Xenopus oocytes. The expressed whole cell currents were measured with a two microelectrode voltage clamp and single channel currents were measured with patch clamp. The chimeric channel adopted both the conductance and the profile for TEA block of the donor NGK2 channel. The exchanged segment seems to incorporate many of the properties of the pore of NGK2. Supported by NIH NS23877 and NS28407.

M-AM-A8

FOUR CLONED K+ CHANNEL SUBFAMILIES ARE INDEPENDENT CURRENT SYSTEMS Manuel Covarrubias[1], Aguan Wei[1], and Lawrence Salkoff[1,2] [1]Department of Anatomy and Neurobiology, [2]Department of Genetics, Washington University School of Medicine, Box 8108, 660 S. Euclid Avenue, St. Louis, MO 63110.

The four *Drosophila* genes, *Shaker*, *Shab*, *Shal* and *Shaw*, are members of an extended gene family encoding potassium channels with distinct functional properties. By coinjection experiments in the *Xenopus* oocyte expression system we show that these four genes code for four independently functioning potassium channel systems. This was shown by expression in *Xenopus* oocytes in all pairwise combinations, as well as by expression of all four channels together. Because of their different kinetics and voltage-sensitive properties each current can be separated from other coinjected partners. In all cases, each expressed current maintains its distinctive properties regardless of whether one or all of the other currents are present. Thus, during coexpression, subunit interaction and assembly occurs independently for each K^+ channel subfamily, and heteromultimeric channels are not formed. This is in contrast to what was recently shown within the *Shaker* subfamily; heteromultimers can form from variant subunits produced by either alternative splicing or different *Shaker* gene products (Christie et al., 1990, Neuron; Isacoff et al., 1990, Nature; Ruppersberg et al., ibid). These *Shaker* heteromultimers form channels with novel properties not seen in homomultimers formed from the same subunits.

Cells *in vivo*, however, clearly require diverse potassium channel systems which function independently of each other. In *Drosophila*, for example, flight muscle cells have an A-current and a delayed rectifier that are separable both genetically and developmentally (Salkoff, 1983, CSHSQB) and thus, are apparently completely independent subsystems. The four cloned K^+ channel subfamilies, *Shaker*, *Shab*, *Shal* and *Shaw*, represent potassium channel systems that are similarly independent of one another.

M-AM-A9

RECOVERY FROM FAST INACTIVATION IN *SHAKER* K^+ CHANNELS IS SPEEDED BY EXTERNAL K^+ AND OFTEN OCCURS THROUGH THE OPEN STATE. Susan D. Demo and Gary Yellen, Howard Hughes Med. Inst., Neuroscience, and Biophysics, Johns Hopkins Sch. of Med. Baltimore, MD 21205

We studied the gating of *Shaker* K^+ channels expressed in transiently transfected 293 cells and in *Xenopus* oöcytes. We found that high external [K^+] increased the rate of recovery from fast inactivation. In high external [K^+] (160 mM) the recovery time course was single exponential, whereas in low external [K^+] (5 mM), recovery was slower and best described by a double exponential. Under all conditions the rate of recovery was voltage-dependent, increasing at more hyperpolarized potentials.

These observations are similar to the effect of external K^+ on internal blockers seen by Armstrong in delayed rectifier K^+ channels. He found that high external [K^+] decreased the affinity of intracellular blockers, and suggested that K ions can effectively "push" the blocker out of the pore through electrostatic repulsion. Hence, our observation that K^+ speeds recovery is consistent with the "ball and chain" model for inactivation as proposed by Armstrong and Bezanilla for voltage-dependent Na^+ channels and by Hoshi, Zagotta, and Aldrich for this *Shaker* K^+ channel, since this model suggests that an internal tethered blocker is responsible for inactivation.

In high external [K^+], it is possible to observe channel openings upon repolarization (tail currents). Following a brief depolarizing pulse, most of the current in the tails arises from channels that were open at the end of the pulse. With longer pulses, we still observe opening events upon repolarization, in spite of the fact that most of the channels have inactivated. Further, we found that the time course of the tail currents parallels the time course of recovery from inactivation. This suggests that channels often open in the process of recovery from inactivation, as though the inactivation particle holds the channel open until it leaves.

M-AM-B1

RESPECTIVE ACTIVATION OF ATP-SENSITIVE AND MUSCARINIC K+ CHANNEL BY PERTUSSIS TOXIN-SUBSTRATE G PROTEIN α AND βγ SUBUNITS IN CARDIAC CELL MEMBRANE.. Robert T Tung[1], Hiroyuki Ito[2], Reiko Takikawa[2], Tsuneaki Sugimoto[2], Ichiro Kobayashi[3], Katsunobu Takahashi[3], Toshiaki Katada[3], Micho Ui[4] and Yoshihisa Kurachi[1,2].
1. Division of Cardiovascular Diseases, Department of Internal Medicine, Mayo Clinic,, Rochester MN 55905, USA; 2. The 2nd Department of Internal Medicine, Faculty of Medicine, University of Tokyo, Hongo, Bunkyo-ku, Tokyo 113, Japan; 3. Department of Life Science, Faculty of Science, Tokyo Institute of Technology, Magatsuda-cho 4259, Midori-ku, Yokohama 227, Kanagawa, Japan; 4. Department of Physiological Chemistry, Faculty of Pharmaceutical Sciences, University of Tokyo, Hongo, Bunkyo-ku, Tokyo 113, Japan.

G proteins couple membrane receptors and various effectors, and play a central role in the transmembrane control of cellular functions. G proteins are dissociated into α-GTP and βγ subunits for their functional regulation of various effectors, including ionic channels. Effects of α-GTP and βγ subunits on K+ channels of guinea-pig cardiac myocytes were examined using the inside-out patch-clamp technique. In ventricular cell, after inside-out patches were formed in internal solution containing 100 μM ATP, 100 pM α_{i1}-GTP-γS, α_{i2}-GTP-γS or α_o-GTP-γS induced bursting openings of a K+ channel, which were suppressed by 2 mM ATP or 1 μM glibenclamide. This K+ channel had a conductance of ~90 pS at a holding potential of -80 mV with slight inward-rectification in the outward direction and a mean open-time of 1.4 ms. Thus, the K+ channel was the K_{ATP} channel. In the presence of 10 μM adenosine in the pipette solution, the GTP-induced K_{ATP} channel openings were inhibited by βγ subunits (10 nM). In atrial myocytes, α_{i1}-GTP-γS (300 pM) caused bursting openings of the K_{ATP} channel in the inside-out patches, but not those of the K_{ACh} channel. In the same patch membrane, however, βγ subunits (10 nM) caused marked openings of the K_{ACh} channel. The K_{ACh} channel had a conductance of 45 pS with a prominent inward-rectification and a mean open-time of 1.1 ms. These observations clearly showed the distinct functional roles of G protein α-GTP and βγ subunits in cardiac myocytes: α subunits are most likely to be the functional arm of G proteins in the K_{ATP} activation in atrial and ventricular cells, while βγ subunits in the K_{ACh} activation in atrial cells.

M-AM-B2

POTASSIUM CURRENTS OF *HERMISSENDA* PHOTORECEPTORS AND RAT SYMPATHETIC NEURONES ARE REDUCED BY A 20kD G-PROTEIN IMPLICATED IN CONDITIONING.
P.L. Huddie, M. Palmatier[1], T.J. Nelson & D.L. Alkon. National Institutes of Health, Park 5, Rm 431, Bethesda, MD 20892, and [1]Cellular Transplants Inc., 4, Richmond Square, Providence, RI 02906.

Associative conditioning of the nudibranch mollusc *Hermissenda crassicornis* produces a reduction of potassium conductances in the Type B photoreceptors; both the early transient K^+ current (I_A) and the Ca^{2+}-dependent K^+ current (I_{KCa}) are affected. In conditioned animals the level of a low (20kD) molecular weight G-protein (cp20) in the Type B photoreceptor is elevated. When injected ionophoretically into the Type B cells small but unquantified amounts of cp20 (< 7.5μg.ml^{-1}) cause depression of I_A and I_{KCa} within 17 minutes after impalement.

The whole-cell patch clamp method permits controlled intracellular dialysis; cp20 extracted from naive *Hermissenda* was dissolved at 500pM concentrations (10ng.ml^{-1}) in Buffer X with 1mM K-ATP and 1mM GTP (for *Hermissenda* experiments) or, for rat neurones, an appropriate intracellular medium with 1mM ATP and 1mM GTP. Patch pipettes of 2-5 MΩ resistance were filled with these solutions. Whole-cell clamped *Hermissenda* photoreceptors exhibited a light-activated inward current; depolarizing command voltages evoked I_A and I_{KCa} which were comparable to the currents obtained with two-electrode voltage clamp, and persisted for 30 minutes during dialysis with boiled cp20 or Buffer X alone; in cp20 treated photoreceptors I_A and I_{KCa} were abolished after 15-20 minutes. Similarly, rat neurone outward currents were reduced within 5 minutes of dialysis, and voltage-dependent inward currents were also inhibited.

M-AM-B3

MODULATION OF MUSCARINIC K+ CURRENT BY PHOSPHORYLATION: MECHANISM OF DESENSITIZATION. Donghee Kim, Department of Physiology and Biophysics, Chicago Medical School, North Chicago, IL 60064

Acetylcholine (ACh) activates the muscarinic-gated K+ current in atrial cells via G protein. After a rapid initial onset, the ACh-evoked current decreases quickly in a biphasic fashion to a near steady-state level after several min. We examined the mechanisms of rapid and slow phases of the K+ current desensitization using neonatal rat atrial cells. In cell-attached patches, ACh (10 μM)-induced desensitization was present in nearly all cells studied. Single channel analyses revealed that the decrease in channel activity was associated with progressive shortening of the mean open time from ~6 ms to ~1 ms over a 20 s period. This suggested that the K+ channel kinetics could be modulated by intracellular second messengers produced by ACh. In inside-out patches, addition of ATP (1 mM) to GTP-activated K+ channels resulted in a progressive increase in mean open time from ~1 ms to ~6 ms and this was Mg^{2+}-dependent, suggesting involvement of a protein kinase. Addition of Ca^{2+} (>10 μM) or alkaline phosphatase (10 units/ml) reversed the effect of ATP on channel kinetics, suggesting involvement of a protein phosphatase. These results indicate that the rapid desensitization is due to modulation of the K+ channel kinetics by phosphorylation and subsequent dephosphorylation of the channel itself or an associated regulatory protein. The slow phase of desensitization was due to a gradual time-dependent decrease in the frequency of channel opening, presumably due to effects on the receptor-G protein coupling. (Supported by NIH and AHA).

M-AM-B4

INTERACTING ACTIONS OF FMRFa AND SEROTONIN ON THE APLYSIA S-K+ CHANNEL. F. Belardetti and R. Shi*. Depts. Pharmacology, *Cell Biology and Neuroscience, Univ. Texas Southwestern Med. Ctr., Dallas, TX 75235.

In Aplysia mechanosensory neurons, serotonin (5-HT) reduces the number of active S-K+ channels (S channels) through cAMP-dependent phosphorylation. The peptide FMRFa: (1) in basal conditions, increases the opening probability of S channels through activation of the 12-lipoxygenase pathway of arachidonate metabolism, and (2) re-opens S-channels closed by cAMP, through an unknown mechanism. We investigated this second action of FMRFa by voltage-clamping sensory cells in culture at -35 mV. Puff applied FMRFa activated an outward current (597 ± 229 pA, 100 μM, mean ± SEM). Bath-applied 8-bromo-cAMP produced an inward current (82 ± 18 pA, 1-10 μM). If FMRFa was applied at 100 μM in the presence of 1-10 μM 8b-cAMP, it produced a larger total outward current (687 ± 245 pA, n=7), equal (on the average but also within each individual cell tested) to the sum of the currents generated by FMRFa and 8b-cAMP alone. Similarly, the current from maximal 8b-cAMP(100 μM, n=3) was completely antagonized by 500 μM FMRFa. In another group of experiments, bath-applied 5-HT at moderate level (10 nM) induced an inward current (39 ± 5 pA). Under these conditions, FMRFa even at supra-maximal concen trations (500 μM), could not completely antagonize the action of 5-HT (total outward current 701 ± 192 pA in the absence, 700 ± 168 pA in the presence of 5-HT, n=7). In light of the 8b-cAMP/FMRFa experiments here presented, this 5-HT effect is not an indication of a non-competitive regulation of the level of phosphorylation of the channel, as suggested by our initial work (Neurosci. Abstr., 794, 1990). Rather, either 5-HT activates an additional cAMP-independent inward current, or it inhibits the opening action of FMRFa on the S channel through an unknown pathway. In summary, the S channel has at least two regulatory sites: the phosphorylation site, competitively controlled by two transmitter pathways and regulating the availability of the channel, and the site for direct binding of a lipoxygenase metabolite, that regulates its opening probability.

M-AM-B5

PTX-RESISTANT G_o EXPRESSED IN PTX-TREATED NG108 CELLS RECONSTITUTES THE INHIBITION BY L-ENKEPHALIN OF $I_{Ca,V}$. Taussig, R., Sanchez, S., Rifo, M., Gilman, A.G., Belardetti, F. (Sponsored by J. Albanesi). Dept. of Pharmacology, UT Southwestern, Dallas, TX 75235.

The transduction of extracellular signals into intracellular responses is mediated in part by a family of G proteins which couple receptors to effector molecules; however, the specificity of G proteins for particular cellular pathways is poorly understood. G_o, an abundant protein in brain, has been proposed to mediate the depression of the $I_{Ca,V}$. We have investigated the role of this G-protein in the cell line NG108, by taking advantage of the properties of pertussis toxin (PTX) which blocks the coupling of receptors to a subfamily of G proteins (G_{i1}, G_{i2}, G_{i3}, G_o, and G_t). The cDNA encoding a PTX-insensitive mutant $G\alpha_o$ subunit was constructed by introducing a point mutation resulting in a cysteine to serine change four residues from the carboxy-terminus. To characterize this protein, this cDNA was expressed in E. coli and the recombinant $G_{o\alpha}$ ($rG_{o\alpha}$) protein purified. The mutant $rG_{o\alpha}$ bound guanine nucleotide and coupled to muscarinic receptors in reconstituted phospholipid vesicles; however, the mutant $rG_{o\alpha}$ labeled in vitro to less than 2% of the level of wild type $rG_{o\alpha}$ in the presence of PTX and ^{32}P NAD. A construct containing a neomycin resistance gene and the mouse metallothionine promoter driving the expression of the PTX-insensitive $G_{o\alpha}$ mutant cDNA was transfected into NG108 cells and antibiotic-resistant clones were isolated. Using western blot analysis, we assayed clones for the expression of the mutant $G_{o\alpha}$. One clone was analyzed by whole cell patch clamp techniques. In wild type NG108 cells, L-enkephalin decreased the $I_{Ca,V}$ (9/10 responsive). After PTX, most cells became insensitive to L-enkephalin (3/9). In the transfected cells, L-enkephalin produced inhibition in all the cells before PTX (6/6), and after PTX (6/6), indicating that the response was reconstituted by the PTX-resistant G_o. We are currently using the same approach to determine whether the muscarinic and α-adrenergic inhibition of $I_{Ca,V}$ in NG108 cells occur via this same pathway.

M-AM-B6

ON THE ROLE OF ARACHIDONIC ACID IN THE ACTIVATION OF 'S'(-LIKE) K CURRENT BY NEUROTRANSMITTERS IN *APLYSIA* NEURONS. V. Březina, Department of Physiology & Biophysics, Mount Sinai School of Medicine, New York.

Recent proposals that lipoxygenase metabolites of arachidonic acid (AA) are the mediators of several *Aplysia* 'slow' 'S'(-like) K-current transmitter responses were based in large part on the ability of AA to mimic and of certain inhibitors of its release and metabolism to block them. I now report results of control experiments (using the K-current responses to FMRFamide, acetylcholine and histamine in neurons R2, LP11, L10 and L2-L6) that put this evidence into perspective: (i), 'S'(-like) K current is easily induced not only by AA, but also by other fatty acids, with effectiveness (at <1-60 μM) roughly proportional to degree of unsaturation (22:6 > AA [20:4] = 18:3 [γ-linolenic] > 18:3 [linolenic] > 22:4 = 20:3 = 20:2 = 18:2), and many non-biological hydrophobic compounds. Effectiveness of exogenous fatty acid or AA metabolite thus cannot, in itself, unambiguously determine its physiological relevance. (ii), each of the (in other preparations very nonspecific) AA-pathway inhibitors BPAB, NDGA, indomethacin, BW755C and ETYA elicits a different subset of several of a spectrum of effects, at least some probably unrelated to AA metabolism. (iii), in particular, the 'fast' Cl-current response to acetylcholine, whose speed and persistence in cell-free patches make it unlikely to be mediated by a second-messenger mechanism, is no less sensitive to the inhibitors than are the 'slow' K-current responses. To begin even the easier task of excluding effects as unrelated to the inhibitors' block of AA-pathway enzymes requires biochemical knowledge of their potency in *Aplysia*. (iv), such data *do* exist for NDGA, which at 3 μM blocks 50%, at 30 μM >98%, of lipoxygenase activity. At precisely these concentrations NDGA activates a large 'S'(-like) K current and initially potentiates, then occludes the transmitter K-current responses. Thus lipoxygenase block may attenuate the responses not by preventing channel opening but, on the contrary, by opening the channels maximally even in the transmitters' absence. Thus, the hypothesis of AA involvement in these responses remains unproven.

M-AM-B7

SINGLE CHLORIDE AND POTASSIUM CHANNELS IN THE EPITHELIAL CELL LINE T_{84}. J.A. Tabcharani and J.W. Hanrahan. Department of Physiology, McGill Univ., 3655 Drummond St., Montreal, Quebec Canada H3G 1Y6

Transepithelial chloride secretion requires the activation of apical Cl and basolateral K conductances however the pathways are not yet well defined at the single channel level. In the apical membrane of T_{84} cells we have studied a Cl channel which differs from those described previously in these cells and which probably mediates secretory Cl efflux (FEBS Letters 270:157, 1990). This low-conductance Cl channel is nearly ohmic (8.7 pS at 37°C), stimulated by cAMP, and apparently insensitive to IAA-94 (100 μM) and DIDS (100 μM). Outward rectifiers coexist in apical membrane patches but they have higher conductance (46 pS), are usually inactive in the cell-attached configuration, and do not respond to cAMP. Transepithelial Cl secretion is stimulated by cAMP and is insensitive to IAA-94 and DIDS, therefore its properties are compatible with the low-conductance Cl channel but not with the outwardly rectifying anion channel. Arachidonic acid activates the low-conductance Cl channel and is much more potent than mixtures containing db-cAMP + IBMX + forskolin. At the basolateral membrane we have identified two types of inwardly rectifying K channel. One has a conductance of 64 pS at hyperpolarizing potentials (pipette [K] = 150 mEq/L), is relatively voltage-independent, and is insensitive to quinidine but blocked by TEA_o. Its activity is transiently increased when cells are exposed carbachol (100 μM) or ionomycin (2 μM). The other basolateral K channel has a conductance of 20 pS under similar conditions, is unaffected by Ca ionophores, and is only observed when cells are exposed to hypotonic solutions. Neither K channel appears to be modulated by cAMP however they may be important during carbachol-induced Cl secretion and cell volume regulation, respectively. Supported by the U.S. and Cdn. CF Foundations and NIH HL41959.

M-AM-B8

MODULATORS OF THE WHOLE-CELL CHLORIDE CURRENT IN A6 CELLS. **Kasama R, Kelepouris E and Agus ZS. Departments of Medicine and Physiology, University of Pennsylvania, Philadelphia, PA 19104.**

Single-channel recordings techniques show that A6 cells, derived from Xenopus laevis, have chloride selective channels which can be activated by cAMP or cytosolic Ca^{2+}. To characterize the regulation of chloride conductance in these cells by protein kinases and divalent cations, single cells were studied in the whole-cell mode.

I_{Cl} (at +60 mV) increased from 5.78±2.24 to 30.2±5.20 μA/cm², as cytosolic free Ca^{2+} ($[Ca^{2+}]_i$) was increased from 0.1-1 μM{p<0.005} and was decreased to 1.67±0.7 μA/cm² in a concentration-dependent manner by increasing $[Mg^{2+}]_i$ from 0 to 10 mM. cAMP (10 μM) increased I_{Cl} from 11.2±3.7 in controls to 38.6±5.8 μA/cm² {p<0.005} while phorbol 12,13 dibutyrate (PE)(10 nM), a protein kinase C (PKC) activator, caused I_{Cl} to decrease (0.59±0.4 μA/cm², p<0.05). Inhibition of phosphorylation with AMP-PNP (5 mM), a non-hydrolyzable ATP analogue, blocked the response to Ca^{2+}, cAMP and PE while leading to an increase in I_{Cl} from 3.51±0.95 to 17.3±4.7 μA/cm² {p<0.01}. H-7, an inhibitor of PKC, reversed the effects of PE (6.7±3.24 μA/cm², p<0.05) and in the absence of PE closely mimicked the effects of AMP-PNP, increasing I_{Cl} to 19.1±4.30 μA/cm², p<0.005. Ca^{2+}, cAMP, AMP-PNP and H7 induced currents were all blocked by increasing $[Mg^{2+}]_i$.

The data indicate that I_{Cl} in A6 cells is regulated by multiple pathways. $[Ca^{2+}]_i$ and cAMP activate I_{Cl} through phosphorylation-dependent pathways and PKC activation inhibits I_{Cl} also requiring phosphorylation. As inhibition of phosphorylation (with AMP-PNP) and PKC (with H7) lead to increases in I_{Cl}, there appears to be a phosphorylation-independent pathway as well as tonic inhibition by PKC. Additional regulation is provided by $[Mg^{2+}]_i$ which inhibits both phosphorylation dependent and independent pathways.

M-AM-B9

PROTEIN KINASE MODULATION OF A CHLORIDE CONDUCTANCE IN CORTICAL THICK ASCENDING LIMB (TAL) CELLS. **E. Kelepouris and Z.S.Agus, Depts. of Medicine and Physiology, Univ. of Pennsylvania, Philadelphia, PA**

Protein kinases modulate ion channel function in a variety of tissues. In this study we addressed their role in the regulation of ion transport in the TAL of the kidney. In previous studies, we have demonstrated the presence of both K and Cl currents in a cell line derived from this kidney segment and have shown a role for cytosolic Mg^{2+} in the regulation of the Cl current. To further characterize I_{Cl}, single cells were studied using the whole-cell patch clamp technique. Internal solutions contained (mM): 120 TEA, 100 aspartate, 20 Cl, 14 EGTA, 5 Mg^{2+}ATP.

In asymmetrical Cl solutions, an outwardly rectifying current was identified with an E_{rev} close to E_{Cl}. Control I_{Cl} (internal solution: 5 mM ATP, 10 nM Ca^{++}) was inhibited by external bumetanide (BUM)(200 μM) from 11±1 to 5±0.4 $\mu A/cm^2$ (at +60 mV) ($p<0.001$), but only minimally reduced by stilbene derivatives. Application of internal cAMP or Ca^{2+} markedly increased BUM-sensitive I_{Cl} (control: 6±0.4; 10 μM cAMP: 16±4 ($p<0.001$ vs. control); 50 μM cAMP: 37±4 ($p<0.05$ vs. control); 200 nM Ca^{2+}: 37±4 ($p<0.001$ vs. control).

Internal phorbol 12,13 dibutyrate(PE)(10nM), an activator of protein kinase C (PKC), increased I_{Cl} to 37±4 ($p<0.05$ vs. control) while internal cGMP (50μM) completely inhibited I_{Cl} (cGMP: 5±0.3; BUM: 5±0.3 $\mu A/cm^2$). Inhibition of phosphorylation with internal AMP-PNP (5mM), a non-hydrolyzable ATP analogue, resulted in complete inhibition of BUM-sensitive I_{Cl} and blocked the activation of I_{Cl} by PE, cAMP, and Ca^{2+}. Internal addition of H-8 (2μM), an inhibitor of protein kinase G, led to an increase in I_{Cl} to 20±4 $\mu A/cm^2$ and prevented the inhibitory effects of cGMP.

Thus, I_{Cl} in TAL cells is Ca^{2+}-activated, BUM sensitive and requires phosphorylation for activation. I_{Cl} appears to be under tonic inhibition by PKG but can be activated via phosphorylation by the cAMP-dependent protein kinases (PKA), PKC or $(Ca^{2+})_i$.

M-AM-B10

PERSISTENT ACTIVATION OF CHLORIDE CURRENT BY GTPγS IN GUINEA PIG VENTRICULAR MYOCYTES

Tzyh-chang Hwang, Minoru Horie and David C. Gadsby (Introduced by Neal Shepherd). *Laboratory of Cardiac Physiology, The Rockefeller University, New York, NY 10021.*

Whole-cell currents were recorded in myocytes voltage-clamped and internally dialyzed with wide-tipped pipettes (~1 MΩ) and an intra-pipette perfusion device. The cells were held at 0 mV and superfused, at ~37 °C, with Ca-free and K-free solution containing 1mM Cd, and usually 1 mM Ba, to minimize Ca- and K-channel currents. With 20 mM Cl and 100 μM GTP in the pipette, and with 150 mM external [Cl], isoproterenol (ISO; 1 μM), forskolin (FSK; 1 μM), or histamine (10 μM) activated an outwardly-rectifying Cl conductance, causing an outward shift of the holding current: these changes were rapidly reversed on washing out the ISO, FSK, or histamine. The response to FSK was identical at 0.1 μM<[FSK]<5 μM and, in the presence of 5 μM FSK, addition of 1 μM ISO caused no further conductance increase. The ISO-activated Cl conductance was abolished completely by propanolol (2 μM), and largely attenuated by acetylcholine (5 μM) or adenosine (10 μM). After switching to pipette solution containing the nonhydrolysable GTP analogue GTPγS (40-100 μM), although FSK-induced currents were still reversible, application of ISO, but not propanolol, caused persistent activation of Cl current which was then insensitive to propanolol, to acetylcholine (up to 15 μM), or to removal of ISO. However, intracellular application of a synthetic peptide inhibitor (100 μM) of cAMP-dependent protein kinase completely abolished the current, and prevented any further response to 1 μM ISO or 1 μM FSK. Similar results were obtained when histamine was used as the activator. When the pipette contained GTPγS and 107 mM Cl, ISO increased membrane conductance as usual, although there was little or no change of holding current at 0 mV. A subsequent switch to pipette solution containing 20 mM Cl caused a large outward shift of the holding current, whether or not ISO was still present. The reversal potentials of the ISO-activated currents were within ~10 mV of estimated Cl equilibrium potentials. The results confirm that ISO and histamine activate Cl conductance through the G_s-mediated activation of adenylate cyclase, and provide no evidence for direct G-protein mediated activation of the Cl conductance. *(Supported by NIH HL-14899 and HL-36783, the Suntory Fund for Biomed.. Research and the Irma T. Hirschl Trust. We thank A. Nairn and P. Greengard for kinase inhibitor.)*

M-AM-C1

Regulation of Smooth Muscle Cytosolic [Ca^{2+}] by Membrane Electrical Events. Peter L. Becker, John V. Walsh, Jr., Joshua J. Singer, and Fredric S. Fay. Dept. of Physiology, Univ Mass Medical Center, Worcester, MA 01655.

Changes in the membrane potential (V_m) represent an important means by which many contractile agents alter the cytosolic [Ca^{2+}]. The relation between [Ca^{2+}], Ca^{2+} current (I_{Ca}) and V_m was studied in single isolated toad gastric smooth muscle cells voltage-clamped with a single microelectrode technique where both I_{Ca} and [Ca^{2+}] were measured simultaneously at msec resolution. Depolarizing command pulses elicited I_{Ca} and a rise in [Ca^{2+}], both of which displayed the same V_m dependence. The amount of calcium that entered through V_m-dependent calcium channels, calculated by integrating the I_{Ca}, exceeded the change in the free internal Ca^{2+} by 150 times, in rough agreement with predictions from measurements of cytosolic calcium buffer capacity. Thus, it would appear that I_{Ca} is sufficient to account for the rise in [Ca^{2+}].

Steady-state "resting" [Ca^{2+}] was found to vary with the holding potential above -40 mV, with a maximum [Ca^{2+}] at -20 mV and lower at more positive or negative V_ms. This observation suggests the presence of a "window" calcium current that elevates the resting [Ca^{2+}] by providing an elevated Ca^{2+} influx. Following a rise in [Ca^{2+}] induced by depolarization, the rate at which the [Ca^{2+}] returned to rest (estimated by measuring time from 70% to 10% of elevated amount) was unaffected by the post-depolarization holding potential over the range of -90 to -50 mV, but was slowed at -30 mV. The V_m dependence of the rate of decline is consistent with the hypothesis that the rate of fall is slowed due to increased Ca^{2+} influx resulting from the window current. To account for these observations, the magnitude of this window current need only be in the range of 4-10 pA. Thus, measurements of [Ca^{2+}] provide a means to study a current that might escape electrophysiological detection at the whole cell level. Finally, these observations provide no evidence for a major role of a Na/Ca exchanger in setting the resting [Ca^{2+}]. Support: NIH HL14523 (FSF), DK31620 (JJS + JVW), AHA Grant-in-Aid (PLB).

M-AM-C2

RELAXATION, $[Ca^{2+}]_i$, AND THE LATCHBRIDGE HYPOTHESIS IN SWINE ARTERIAL SMOOTH MUSCLE. Christopher M. Rembold, Div. of Cardiology, Dept. of Internal Medicine, Univ. of Virginia, Charlottesville, Virginia 22908 USA

During vascular smooth muscle relaxation, myosin light chain phosphorylation values decrease to resting values more rapidly than stress. Since phosphorylation is proportionally low, the latchbridge hypothesis predicts that stress during relaxation should be predominantly carried by latchbridges. I evaluated the mechanical properties of latchbridges by changing tissue length and measuring myoplasmic [Ca^{2+}] with aequorin and stress during relaxation of swine carotid media. The latchbridge model of Hai and Murphy was used to predict stress based on changes in aequorin-estimated myoplasmic [Ca^{2+}]. Relaxation was associated with a large increase in the predicted fraction of stress maintained by latchbridges. The time course of relaxation in swine carotid artery was not substantially altered when the tissue was either briefly stretched or shortened and then returned to the original length. Small increases in [Ca^{2+}]-dependent phosphorylation were able to predict stress redevelopment after the length change except during the first few seconds after stretch. A linear relationship between aequorin-estimated myoplasmic [Ca^{2+}] and stress redevelopment rates was found. These data suggest that latchbridge reattachment either occurs very slowly or does not occur in swine carotid media.

Rapid stretching of smooth muscle induces a large increase in stress (resistance to stretch: RTS), and stress gradually decreases to intermediate values (stress relaxation: SR). In tissues activated with contractile agonists, both RTS and SR appeared to correlate with the stress present prior to stretch, not the magnitude of the stretch-induced [Ca^{2+}] transient. In the unstimulated swine carotid, RTS and SR were independent of $[Ca^{2+}]_o$ and $[Ca^{2+}]_i$, suggesting that RTS and SR in unstimulated tissue were predominantly dependent on the passive components of smooth muscle rather than attached, Ca^{2+}-dependent cross-bridges. Supported by the Markey Trust & NIH HL38918.

M-AM-C3

G-PROTEIN-COUPLED MODULATION OF CA^{2+}-SENSITIVITY IN SMOOTH MUSCLE

T.Kitazawa, B.D.Gaylinn, G.H.Denney and A.P.Somlyo
From the Department of Physiology, University of Virginia, Charlottesville, VA 22908

The Ca^{2+}-sensitivities of tonic (pulmonary and femoral artery) and phasic (portal vein and ileum) smooth muscles and the effects of GTPγS and agonists on the Ca^{2+}-sensitivity of force and myosin light chain (MLC) phosphorylation were determined in α-toxin-permeabilized preparations. The Ca^{2+}-sensitivity of force was higher in the tonic than in the phasic smooth muscles. α_1-adrenergic and muscarinic agonists and guanine nucleotides increased MLC phosphorylation and contractile responses to constant [Ca^{2+}], and shifted their Ca^{2+}-sensitivities to the left. GTPγS significantly increased both MLC phosphorylation and maximum force at pCa5 in the phasic, but not in the tonic smooth muscle. GDPβS reversibly inhibited the agonist-induced Ca^{2+}-sensitization of MLC phosphorylation and force. The lower effectiveness of GTP (app. Km≥10μM) than of GTPγS (app. Km=0.1μM) suggests that Ca^{2+}-sensitization is mediated by a genuine G-protein with GTPase activity. The major results support the hypothesis[1] that the G-protein coupled Ca^{2+}-sensitizing effect of agonists on force development is secondary to increased MLC phosphorylation, possibly through inhibition of MLC phosphatase(s). 1) Somlyo et al. Adv. Protein Phosphatases 5, 181-195 (1989). Supported by HL15835 to the Pennsylvania Muscle Institute and P01 HL19242-14 to the University of Virginia.

M-AM-C4

CONTRIBUTIONS OF MYOSIN LIGHT CHAIN KINASE AND PROTEIN KINASE-C TO ACTIVE INTRINSIC TONE IN VASCULAR SMOOTH MUSCLE.

John Pawlowski and Kathleen G. Morgan. Harvard Medical School, Boston, MA 02215

To investigate the mechanism by which vascular smooth muscle generates active intrinsic tone, we measured the associated myosin light chain (MLC) phosphorylation. We have previously found cooling to be the most effective method to abolish intrinsic tone. Strips of ferret aorta without endothelium were placed in either calcium (Ca^{2+})-containing or Ca^{2+}-free solution. The muscle strips at 37°C showed a baseline level of phosphorylation of 9.09±0.70% mol Pi/mol MLC (n=9). Cooling to 21°C caused no significant change (10.99±1.53%, n=10) whereas further cooling to 0°C reduced significantly the level to 5.90±0.53%, n=4 ($p<.02$). We have previously shown that there is no significant change in $[Ca^{2+}]_i$ with temperature. Ca^{2+}-free bathing media had no significant effect on MLC phosphorylation at any temperature. Another kinase system, protein kinase-C, was investigated using the inhibitory compound, staurosporine (ST). After pretreatment with a maximally-effective dose of ST (10^{-6}M), intrinsic tone was inhibited by 29.5±5.6% (n=9). In contrast, ST reduced phenylephrine contractions by 75.0±2.3% (n=6) and phorbol ester contractions by 97.8±1.4% (n=7).

We conclude that active intrinsic tone in vascular smooth muscle is associated with a change in MLC phosphorylation but in a functionally Ca^{2+}-independent manner. Our experiments using ST also suggest a role for protein kinase-C. We postulate that a significant phosphorylation of the MLC occurs in the resting muscle either through the activity of a Ca^{2+}-independent form of MLC kinase or through ongoing activity of the kinase at resting $[Ca^{2+}]_i$. (Support: HL-31704 and HL-42293 to KGM, GM-07592 to JP)

M-AM-C5

MODIFICATION OF MYOSIN LIGHT CHAIN PHOSPHORYLATION IN K^+-INDUCED SUSTAINED ARTERIAL MUSCLE CONTRACTION BY PHORBOL DIBUTYRATE.

K. Bárány, A. Rokolya, T.S. Guzeman, and M. Bárány. Departments of Physiology and Biophysics and Biochemistry, College of Medicine, University of Illinois, Chicago, IL 60612.

It is known that phosphorylation of the 20 kDa myosin light chain (LC) decreases during sustained K^+-contraction of arterial smooth muscle. We have found that this dephosphorylation of LC can be prevented by addition of phorbol dibutyrate (PDBu) into the bath of the K^+-contracted muscle at 2 min. This phenomenon was investigated by phosphopeptide analysis in order to identify the enzymes involved in the phosphorylation of LC. Recently, we observed (Bárány et al., BBA 1035, 165, 1990) that in a 1 to 2-min K^+-contracted muscle, about 95% of the peptides were phosphorylated by myosin light chain kinase (MLCK) and about 90% of the phosphate was incorporated into a serine residue. Essentially, the same phosphopeptide pattern was found in 60-min K^+-contracted muscle. On the other hand, in 60-min PDBu-contracted muscle 25-40% of the phosphopeptides were attributed to protein kinase C (PKC) phosphorylation and 60-75% to MLCK phosphorylation. When the muscle was treated with K^+ for 2 min and subsequently with K^+ and PDBu for 60 min, LC phosphorylation was much higher than in muscles treated with K^+ alone for 62 min or with PDBu alone for 60 min. Both MLCK- and PKC-induced phosphorylations contributed to this higher level. Furthermore, the pattern of MLCK-catalyzed phosphorylation changed so that instead of a selective serine phosphorylation, considerable threonine phosphorylation occurred as well. Such a switch from serine to threonine phosphorylation in K^+-PDBu treated muscle could be reproduced in vitro: LC was first phosphorylated by PKC and subsequently by MLCK. The results indicate an interrelationship between PKC and MLCK phosphorylated sites of LC in intact arterial smooth muscle. (Supported by AHA and NIH, AR 34602).

M-AM-C6

THE ROLE OF POTASSIUM CHANNELS IN THE RELAXATION OF DISTAL CIRCULAR SMOOTH MUSCLE OF THE RABBIT COLON INDUCED BY PHOTOLYTICALLY RELEASED cAMP. RF Willenbucher, J Vergara, WJ Snape, Jr., Harbor-UCLA Medical Center, Torrance, CA and Dept. of Physiology, UCLA, Los Angeles, CA.

Rapid photolytic release of intracellular cAMP relaxes distal circular muscle (DCM) of the rabbit colon in a dose-dependent manner. Previous experiments suggest sarcolemmal Ca^{2+} transport via the Ca^{2+} pump (Ca^{2+}-dependent ATPase) plays an important role in cAMP-mediated relaxation of DCM. The specific aim of this study was to evaluate the role of sarcolemmal potassium channels in cAMP-induced DCM relaxation. DCM strips from New Zealand White rabbits were incubated in the P-1-(2-nitrophenyl)-ethyl ester of cAMP (caged cAMP)(200uM) for 30 min. The strips were contracted with either bethanechol (10uM) or KCl (80mM). Photolytic release of cAMP by a 1/2 sec exposure to UV light (280-400nm) produced a 91% relaxation of bethanechol-contracted DCM while the same exposure produced only a 25% relaxation of K^+-contracted DCM. This suggested that K^+ channels may play a role in cAMP-mediated relaxation. To test this hypothesis, muscle strips were incubated for 1/2 hour in glybenclamide (10uM)(K_{ATP} blocker), charybdotoxin (ChTX)(4-40nM)($K_{Ca^{2+}}$ blocker), or tetraethylammonium chloride (TEA)(10mM) (nonspecific K^+ blocker at 10mM) prior to bethanechol contraction and flash photolysis. K^+ channel blockade had no effect on cAMP-mediated relaxation of bethanechol-contracted DCM. These studies suggest that: 1) cAMP-mediated relaxation of bethanechol-contracted DCM does not involve the modulation of K_{ATP} or $K_{Ca^{2+}}$ channels, and 2) the difference in relaxation of bethanechol or K^+-contracted DCM may be related to cAMP modulation of the intracellular Ca^{2+} pool.

M-AM-C7

MYOSIN PHOSPHORYLATION AND REGULATION OF CROSS-BRIDGE CYCLING IN NORMAL AND COLITIC COLON SMOOTH MUSCLE. YN Xie, WT Gerthoffer, SN Reddy, WJ Snape Jr., Harbor-UCLA Medical Center and the Inflammatory Bowel Disease Center, Torrance, CA and the Department of Pharmacology, University of Nevada School of Medicine, Reno, NV.

The aims were to test the hypotheses that 1) phosphorylation of the 20 KD myosin light chains (LC-20) in rabbit colon smooth muscle modulates actin myosin cross-bridge kinetics and isotonic shortening velocity, and 2) abnormal LC-20 phosphorylation decreases colonic muscle contractility in colitis. Experimental colitis was induced in New Zealand White rabbits by intrarectal administration of formalin and intravenous immune complexes. Phosphorylated 20 KD myosin light chain was measured using an immunoblot method 5 - 360 sec after 10^{-5}M bethanechol stimulation. Isometric force and the maximal velocity of shortening (Vmax) (isotonic quick release, Cambridge 300B Dual Mode Servo System, controlled by an IBM PC AT computer) were measured in distal circular colonic muscle strips from healthy and colitis rabbits, 13 - 68 sec after 60mM KCl stimulation. Phosphorylation of LC-20 in resting muscle ($18.6\pm1.7\%$) was similar in both groups ($p>0.05$). In healthy rabbits maximal phosphorylation of LC-20 ($33.6\pm3.2\%$) occurred within 15 sec of the stimulation. In tissues associated with colitis, the phosphorylation ($20.7\pm5.2\%$) was delayed to 180 sec ($p<0.01$). In healthy rabbits the Vmax (0.14 ± 0.02 L_o/sec) peaked at 13 sec and isometric stress reached maximum by 38 sec. In muscle from colitic animals the Vmax (0.07 ± 0.01 L_o/sec) was lower ($p<0.01$) and peaked at 18 sec. The LC-20 phosphorylation 5 - 60 sec after muscle stimulation was significantly ($p<0.05$) less in colitis than in normal controls. LC-20 phosphorylation and Vmax decreased rapidly in normal rabbits upon reaching peak isometric stress. These studies suggest that 1) the level of myosin light chain phosphorylation in normal colonic smooth muscle is related to the maximal velocity of shortening rather than to the amplitude of isometric stress, and 2) the maximal shortening velocity and the 20 KD myosin light chain phosphorylation in colitis are decreased.

M-AM-C8

THE EXCHANGE OF THE 20 KDA MYOSIN LIGHT CHAIN-BOUND PHOSPHATE DURING SUSTAINED CONTRACTION OF ARTERIAL MUSCLE. A. Rokolya, K. Bárány, and M. Bárány (Sponsored by M.C. Rao). Departments of Physiology and Biophysics and Biochemistry, College of Medicine, University of Illinois, Chicago, IL 60612.

Sustained arterial muscle contraction is characterized by a low tension cost which may be related to a reduced cyclic phosphorylation and dephosphorylation of the 20 kDa myosin light chain (LC). In order to answer the question whether or not a cyclic phosphorylation-dephosphorylation of LC takes place during the sustained contraction we have studied the exchangeability of LC-bound phosphate during prolonged K^+-induced contraction. K^+-contracted arteries, containing nonradioactive phosphorylated LC, were exposed to carrier free [^{32}P]orthophosphate in K^+-stimulating physiological salt solution during the sustained contraction at 37°C for various times. In control experiments resting arteries, containing mainly dephosphorylated LC, were exposed to carrier free [^{32}P]orthophosphate in normal physiological salt solution at 37°C then contracted by K^+ to produce LC containing radioactive phosphate and left in the sustained contraction state for various times. Arteries were frozen in liquid nitrogen, pulverized, and homogenized in perchloric acid. After centrifugation the supernatant was used for determination the specific radioactivity of [^{32}P] phosphocreatine which is equal to that of [γ-^{32}P] phosphate of ATP, whereas the residue was used to isolate LC by 2D gel electrophoresis. The incorporation of [^{32}P]phosphate into LC was calculated from the total protein applied onto the gels, the counts in LC of the digested gels, and from the specific radioactivity of the [^{32}P]phosphocreatine in the muscle. No difference was found in the [^{32}P] content of LC between muscles which were labeled with ^{32}P in K^+-contracted state and muscles which were labeled in the resting state and then contracted by K^+. This provides evidence for the following reactions in K^+-contracted and ^{32}P-exposed muscles:

$$\text{LC - P} \xrightarrow{\text{MLCP}} \text{LC + P}$$

$$\text{LC + [}\gamma\text{-}^{32}\text{P] ATP} \xrightarrow{\text{MLCK}} \text{LC - }^{32}\text{P + ADP}$$

Thus, a part of the energy consumption during sustained contraction is due to the turnover of the LC-bound phosphate. (Supported by NIH, AR 34602 and AHA).

M-AM-C9

TIME-RESOLVED X-RAY DIFFRACTION MEASUREMENTS ON A LIVING CONTRACTING MAMMALIAN SMOOTH MUSCLE.

A. Arner, Dept. Physiol, Lund, Sweden, G. Rapp, EMBL-Outstation, DESY, Hamburg and J.S. Wray, Max Planck Institute, Heidelberg, Germany.

Understanding smooth muscle contraction involves consideration not only of changes in cross-bridge structure but also of assembly/disassembly of the myosin filaments. In rabbit rectococcygeus (RC) muscles we have shown a 145 Å X-ray reflection from myosin, which became weaker in rigor compared to the relaxed state (Arner et al. 1988; In: Sarcomeric and non-sarcomeric muscles, Ed. U. Carraro; Unipress Padova, p. 699). To further characterize this reflection we measured its intensity during contraction and relaxation. Living RC muscles were electrically stimulated at 22°C, and X-ray patterns recorded using synchrotron radiation. By summing 6-10 cycles a time resolution of 250 ms was achieved. The 145 Å reflection weakened during force development and recovered during force decline; since force production presumably involves assembly rather than disassembly of filaments, this change suggests that cross-bridges move from their ordered arrangement on the thick filaments during force development in smooth muscle, as has been described for some striated muscles.

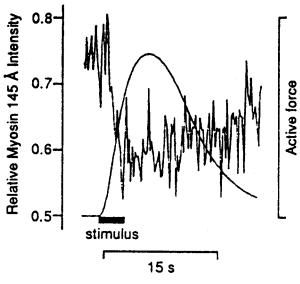

M-AM-D1

AN OPTIMIZATION STUDY OF THE VOLTAGE SENSITIVE GATE IN ION CHANNELS. N.G. Greeff, Physiologisches Institut, Universität Zürich, CH-8057, Switzerland.

The voltage sensor of voltage gated ion channels is known to consist of charged amino-acids. It may be seen as one part of a molecular mechanical device that is driven by the transmembranal electrical field and converts electrical force into mechanical force in conjunction with the other part, the actual gate. There are five charged residues available: Arg^+, Lys^+, His^+, Glu^- and Asp^-. Taking into account their different molecular dimensions, it was studied how efficiently each residue would perform when used in a certain molecular gating device. In particular, in the sliding helix model the transmembranal segment S_4 in α-helical conformation would form a screw with 3 ridges embedded between the adjacent segments of the channel. This allows and defines a screw-like motion of 60^o per 4.5 Å axial movement. Also taking into account the radial distance from the helix axis of the charge in the residue, the relative fractions of force vectors acting upon the helix are derived. From 3-D molecular graphics, the geometrical data for the quantitative analysis were obtained and the torque momentum and the axial force component derived. It is found that the long residues Arg^+ and Lys^+ would produce significantly more torque momentum than the longest negative residue Glu^- while, in contrast, the axial force component would be larger for the shorter residues. Since it is known that evolution has chosen the long positive residues for the voltage sensor with a predominance of about 3:1 for Arg^+:Lys^+ it is concluded that this reflects an evolutionary optimization of a sliding helix as the gating device which uses torque force rather than force in axial direction of the helix.

M-AM-D2

THE HIGH-TEMPERATURE CAPACITANCE RISE IN AXON MEMBRANES IS CONSISTENT WITH A FERROELECTRIC CURIE-WEISS LAW FOR Na CHANNELS. H. Richard Leuchtag, Materials Research Laboratory, Pennsylvania State University; permanent address, Department of Biology, Texas Southern University, Houston, TX 77004.

A consequence of the ferroelectric-superionic transition hypothesis (Leuchtag, J. Physiol. 418:10P, 1989; Proceedings, Int. Symp. on Appl. of Ferroelectrics, IEEE, 1990) for voltage-gated Na channels is that their dielectric permittivity ϵ must obey a Curie-Weiss law, $\epsilon = B/(T_C - T)$ below the Curie temperature T_C, identified at rest potential as the heat-block temperature. With bilayer capacitance C_0, ratio of channel pathway area to membrane area a and membrane thickness L, the membrane capacitance per unit area becomes $C = C_0 + b/(T_C - T)$, where $b = \epsilon_0 aB/L$. This relation was fitted to C versus T data obtained from Loligo pealei by Palti and Adelman (J. Memb. Biol. 1:431, 1969) with parameters $C_0 = 1.15\ \mu F/cm^2$, $T_C = 49.85\ ^oC$ and $b = 2.45\ ^oC\ \mu F/cm^2$. Estimates of $a \approx 0.005$ and $L \approx 40$ Å yield a value for $B \approx 2200\ ^oC$. This is consistent with an order-disorder ferroelectric transition in the channel (Lines and Glass, Principles and Applications of Ferroelectrics, Clarendon, Oxford, 1977). Below T_C the pathway has an ordered structure with two stable polarization states: polarization vector directed inward (excitable) or outward (inactivated). Above T_C the structure is disordered and a superionic conductor of Na^+. The lowering of T_C by depolarization accounts for voltage-dependent gating.

M-AM-D3

KINETICS OF THE FAST COMPONENT OF CHARGE MOVEMENT IN THE SQUID.
I.C. Forster and N.G. Greeff, Physiologisches Institut,University of Zürich, CH-8057,Switzerland.

Using a fast low-noise voltage clamp system (J.Neurosci. Meth.,33, 185-205) we have resolved a displacement charge component which moves independently of the main Na channel gating charge (PNAS,1990, in press). Specific voltage step protocols, designed to minimise contamination of the fast charge from slower components, have enabled accurate separation of this component (Biophys. J.,57,105a). Kinetic analysis of these data confirms that this component can be modelled as a single step process obeying Eyring-Boltzmann kinetics with a quantal charge of up to 1.2 e^-, a highly asymmetrically positioned barrier and a total charge movement between saturation limits of about 2 nC cm^{-2}, lying in the voltage range associated with normal Na channel gating. We have no direct evidence that this component is part of the Na channel gating process, however if this were the case, these data would be consistent with there being one fast gating unit per channel, assuming a Na channel density of 180 μm^{-2} (J.Physiol,377,463-486). Furthermore, the kinetic independence of the fast component permits its direct subtraction from the main gating charge thus helping to elucidate the true initial time course of the latter. Supported by Swiss NF grant 3.143-0.85.

M-AM-D4

EXTRACTING RATE CONSTANTS FROM DATA. A PRACTICAL METHOD, L. Goldman (Intro. by D.R. Matteson), Dept. of Physiology, School of Medicine, Univ. of Maryland, Baltimore, MD 21201.

First consider $C_1 \underset{k_{12}}{\overset{k_{21}}{\rightleftarrows}} C_2 \underset{k_{23}}{\overset{k_{32}}{\rightleftarrows}} O_3$. Occupancy of the open state is $P_3(t)=P_3(\infty)-[(P_3(0)+b(P_3(0)-P_3(\infty))/(a-b)]\exp(-at)+[(P_3(0)+a(P_3(0)-P_3(\infty))/(a-b)]\exp(-bt)$, with $a,b=(k_{21}+k_{12}+k_{32}+k_{23})/2 \pm [((k_{21}+k_{12}+k_{32}-k_{23})/)^2+k_{32}(k_{23}-k_{21})]^{1/2}$, $P_3(\infty)=k_{21}k_{32}/((k_{21}k_{32}+k_{21}k_{23}+k_{12}k_{23})$, and $P_3(0)=-k_{23}P_3(0)+k_{32}P_2(0)$. $P_3(0)$ and $P_2(0)$ are initial occupancies of O_3 and C_2. 5 values are obtained from the current time course during a step in potential ($a,b,P_3(\infty)$, $P_3(0),P_3(0)$) and 6 values are needed (4 k_{ij}'s and 2 initial conditions). Each additional potential from the same initial conditions provides 4 new values and introduces 4 new unknowns. Noting that $k_{ij}=\exp[A_{ij}+B_{ij}V]$ provides no additional measurable quantities and so can never produce a unique solution (Balser, Roden and Bennett, Biophys. J.57:433-444,1990). To solve the problem record currents at any 2 potential steps,V and V_c,from the same initial conditions, giving 9 values for the 10 unknowns. Now step to V_c for time T and then to the original V. The state occupancies are continuous. $P_2(0)(\text{at } V)=P_{c2}(T)$ (at V_c) and similarly for P_3. Without loss of generality T can be steady state yielding $P_3(0)/P_{c3}(\infty)=k_{c23}(k_{32}/k_{c32})-k_{23}$. $P_3(0)$ from V following V_c is a new experimental value not predictable from the currents at V and V_c separately as it includes the effect of the unknown P_2 variable. No new unknowns are introduced. Solving simultaneously the expressions for $a,b,P_3(\infty),P_3^*(0)$ (the star indicates a step from reference) and the measurable $P_3^*(0)$, an analogous set for V_c (from reference) and $P_3(0)/P_{c3}(\infty)$(at V following the step to V_c) provides a solution with 2 roots. The method is valid when $P_3^*(0)=0$, but if $P_3^*(0)=P_2^*(0)=0$,2 durations of V_c are needed. Similarly, a solution is obtained from the current during a single step at ON and the tail current at OFF, but only if the potential preceding and following the step are the same and $P_3^*(0),P_2^*(0)\neq 0$. Any number of states can be solved in certain special cases, e.g. for $C_n \rightleftarrows C_{n-1} \cdots C_3 \rightleftarrows C_2 \rightleftarrows O_1$, as enough durations of V_c are always available. Supported by N.I.H. grant NS07734.

M-AM-D5

SINGLE SODIUM CHANNELS IN HIGH INTERNAL SODIUM IN THE SQUID GIANT AXON. Francisco Bezanilla and Ana M. Correa. Department of Physiology, UCLA, Los Angeles, CA 90024.

Previous studies on perfused squid axons with high internal sodium showed that the Na^+ current at positive potentials exhibit incomplete inactivation. It has been proposed that the time course of the Na^+ current under these conditions could be the result of two types of sodium channels, the normal inactivating type and a non-inactivating type. To extend the voltage range of sodium channel kinetics we studied the single channel characteristics in squid axons with high internal sodium using the cut-open axon technique. The external solution contained 270 mM Na^+ and the internal solution had 535 mM Na^+. We studied the kinetics of activation in the voltage range from 40 to 120 mV. The averaged currents rise rapidly to a peak and then inactivate incompletely, as has been described for the perfused axon. The degree of incomplete inactivation is increased with more depolarization.

In a single channel patch, at 110 mV the ratio of peak to steady current (for an 18 ms pulse) was about 3. The peak probability was 0.65 and was approximately constant between 60 and 110 mV. The channel opened early after pulse onset and reopened many times for pulses of 18 ms long. In traces with at least one opening, the number of openings per trace averaged 10. These reopenings accounted for the non-inactivating portion of the Na^+ current. The distribution of open times showed two clear components at all the potentials studied. The first latency distributions showed also two components: a very fast component (less than 1 ms) accounted for about 90% of the first latency and a much slower component for the rest. These results show that with high internal Na^+ and at very positive potentials, squid axon sodium channels have two open states. Our results show that only one type of Na^+ channel accounts for incomplete inactivation of Na^+ currents at positive potentials because the average current was the result of only one active channel in the patch. Supported by USPHS grant GM30376.

M-AM-D6

MODIFICATION OF Na^+ CHANNELS BY PRONASE, NBA AND TMO. Ana M. Correa and Francisco Bezanilla. Department of Physiology, UCLA, Los Angeles, CA 90024

To gain further insight into the mechanisms underlying sodium channel inactivation and deactivation, the single channel activity of squid Na^+ channels was studied before and after modifications by brief exposures of the internal surface of cut-open axons to the action of the proteolytic enzymes in *pronase*, and chemical modifiers such as *N-bromoacetamide* (NBA) and *trimethyloxonium* (TMO). The single channel conductance and the mean open time (MOT) of the unitary events were measured in a normal voltage range using 540 mM Na^+ outside and 50 mM Na^+ inside (with Cs^+ as the main internal cation) or in extended voltage ranges achieved by varying the Na^+ gradient either by increasing the external Na^+ to 4 M or by using higher internal Na^+ concentrations (107 and 205 mM Na^+, with no other cationic substitute). As expected, pronase and NBA eliminated fast inactivation as seen in the average accumulated currents without a clear alteration of the activation kinetics. At the single channel level these reagents had no measurable effect on the single channel conductance. In 4 M external Na^+, pronase did not affect the MOT of the channel in a range from -40 mV to +40 mV. Conversely, under normal gradient conditions (540//50) pronase increased the MOT in a voltage range from -60 to 0 mV. Under similar ionic conditions a small increase in MOT was observed in NBA treated channels. The lack of macroscopic inactivation due to pronase and NBA is primarily due to multiple reopenings of the channels during the depolarizing pulses. A preliminary analysis of the effects of TMO showed no evident alteration of the kinetics of the reconstructed macroscopic currents. It did, however, produce saturation of outward currents. After TMO treatment the current-voltage relations showed varying degrees of rectification at potentials more positive than the Na^+ reversal potential. The effect of TMO on the conductance could be interpreted as the result of a reduction of negative charge in the inner mouth of the channel. Supported by USPHS grant GM30376.

M-AM-D7

FAST AND SLOW COMPONENTS IN MYXICOLA AXON GATING CURRENTS. L. Goldman, Dept. of Physiology, School of Medicine, Univ. of Maryland, Baltimore, MD 21201.

ON gating current (I_{ON}) in Myxicola axons under series resistance compensation peaks in 20-35μs, 4 to 6 fold faster than previously reported (e.g. Schauf, Eur. J. Pharm. 136:89-95,1987), and is not a single exponential. Pooled values of τ_{ON-F} (6 axons) increased from 50-82μs at +70mV to 126-199μs between +30 and -10mV, and decreased again at more negative potentials. τ_{ON-S} increased from 249-520μs at +70mV to 531-779μs between +30 and 0mV, and also decreased at more negative potentials. These values are indistinguishable from these in squid axons. In a typical record the usual 2-exponential fit started at either 75 or 125μs extrapolated well through the peak at 30μs, suggesting full settling of the clamp by this time, and providing no indication of an additional very fast relaxation. Fast and slow components are also seen in I_{OFF} at -100mV. Neither of these reflect recovery from charge immobilization as the I_{OFF} integral, Q_{OFF}, is clearly less than Q_{ON} even when both components are included. Deactivation of the 2 I_{ON} components seem to be well separated. Na tail currents also show 2 components (plus a third very small and slow relaxation from a second small sub-population of Na channels). At -100mV, means for Na tail time constants (4 axons) are 76μs (range:53-89 μs) and 344μs (range:312-387 μs), and for I_{OFF} (6 axons) 62μs (range:34-87μs) and 291 μs (range:204-456μs) in reasonable agreement. I_{Na} activation (τ_A) and I_{ON} kinetics do not agree. τ_A is slower than τ_{ON-F} at all potentials. τ_{ON-F} may reflect the process(es) delaying the rise of I_{Na}. Except for a brief overlap range between -30 and -15mV, corresponding to the intermediate component of Armstrong and Gilly (J. Gen. Physiol. 74:691-712,1979), τ_{ON-S} is too slow to be Na activation and too fast to be inactivation. From -30 to 40 mV τ_A decreases while τ_{ON-S} either increases with or is independent of potential. In the overlap region τ_A decreases while τ_{ON-S} increases with potential. There is a process in the gating current not corresponding to any known I_{Na} process and no gating current process corresponding to Na activation. Supported by N.I.H. grant NS07734.

M-AM-D8

MODELING NA AND GATING CURRENTS. L. Goldman (Intro. by K.A. Gregerson), Dept. of Physiology, School of Medicine, Univ. of Maryland, Baltimore, MD 21201.

Available Myxicola Na and gating current data provide no direct evidence for more than 2 closed states. Na activation and gating current (I_g) were then modeled by a $\text{closed}_2 \underset{k_{12}}{\overset{k_{21}}{\rightleftharpoons}} \text{closed}_1 \underset{k_{01}}{\overset{k_{10}}{\rightleftharpoons}} \text{open}$ scheme. Analytical solutions were used to distinguish inherent properties from those dependent on selected parameters. All ON results are with initial occupancy of closed_2=1.0, and OFF with that for open=1.0. At ON for the closed_2-closed_1 transition $I_{g21}(t)=k_{21}Q_{21}N[((k_{21}+k_{12}-b)/(a-b))\exp(-at)-((k_{21}+k_{12}-a)/(a-b))\exp(-bt)]$, and for the closed_1-open $I_{g10}(t)=k_{10}Q_{10}N[(-k_{21}/(a-b))\exp(-at)+(k_{21}/(a-b))\exp(-bt)]$, where Q_{21} and Q_{10} are charge displaced for each indicated channel transition and N is channel density. $I_g(t)=I_{g21}(t)+I_{g10}(t)$. For $I_{Na}(t)$ see e.g. Goldman (Quart. Rev. Biophys. 9:491-526, 1976). We find:(1) The same relaxations are in $I_{Na}(t)$ and $I_g(t)$, but their relative amplitudes can differ. (2) The number of prominent relaxations in $I_g(t)$ can be greater than the number of transitions with charge displacement. (3) Transitions with substantial charge displacement can be negligible in $I_g(t)$ if the forward rate constant is small. (4) $I_{Na}(t)$ is sensitive to closed state transitions. (5) The presence or absence of an I_g rising phase even if not artifactual provides no unambiguous information about the rate constant order. (6) When the steady state occupancy of open=1.0, $I_{Na}(t)$ is always insensitive to forward rate constant order. (7) When the steady state occupancy of open <1.0, $I_{Na}(t)$ can be more or less sensitive to order depending on the values selected. (8) $I_g(t)$ at OFF always decays as 2 exponentials. (9) More than one relaxation in I_{Na} tail currents does not require more than one open state. When the steady state occupancy of open is not at or near zero during the post pulse, there are always 2 relaxations in I_{Na} tail currents. When the occupancy is zero there are either one or two depending on whether k_{10} or k_{21} is zero. Myxicola tail currents are consistent with $k_{01}>k_{12}$ based on the relative amplitudes of the 2 relaxations. Supported by N.I.H. grant NS07734.

M-AM-E1

INTRACELLULAR Ca^{2+} SIGNALLING IN A PLASMACYTOMA CELL LINE. Michael D. Cahalan[1] and Daniel Choquet[2]. [1]Dept. Physiology & Biophysics, UCI, Irvine, CA 92717; [2]Laboratoire de Neurobiologie Cellulaire, Institut Pasteur, Paris, France; Abt. Membranbiophysik, Max Planck Institute, Göttingen, Germany.

Using whole-cell patch-clamp and fura-2 fluorescence ratio measurement of $[Ca^{2+}]_i$, we have investigated intracellular Ca^{2+} release in RPC 5.4 cells. These cells are believed to represent a late stage in the maturation of B lymphocytes to antibody-secreting plasma cells. The fura-2 ratio and the presence of a voltage-independent, Ca-activated K^+ current simultaneously indicated increases in $[Ca^{2+}]_i$ in response to several experimental stimuli. Dialysis with 10 uM IP3 caused Ca^{2+} release immediately after break-in to achieve whole-cell recording, while 0.1 mM GTPγS caused Ca^{2+} transients after an initial delay averaging 100 sec. Surprisingly, simple and commonly-used pipette solutions containing large anions that are usually impermeant through Cl^- channels (glutamate, aspartate, gluconate, and HEPES) also tended to produce transients after an average delay of ~60 sec. The occurrence of Ca^{2+} transients was independent of membrane potential and extracellular Ca^{2+}, indicating release from an internal store. During prolonged whole-cell recording with pipette solutions containing glutamate or following patch withdrawal, $[Ca^{2+}]_i$ often oscillated with an average period of ~130 sec. Ca^{2+} transients occurred in roughly 80% of cells dialyzed with glutamate, but in only 10% of cells dialyzed with Cl^-. Dialysis with NO_3, SCN, $MeSO_4$, or SO_4, anions which pass through some types of Cl^- channels, also did not result in Ca^{2+} release. Combining glutamate and Cl^- in varying proportions showed that a glutamate/Cl^- fraction between 0.1 and 0.5 is necessary to support Ca^{2+} transients. Addition of 20-1000 uM DIDS to the Cl^- pipette solution also produced Ca^{2+} transients. From these results we propose that Cl^- channels in an intracellular compartment may regulate Ca^{2+} release. We thank Erwin Neher and the Alexander von Humboldt Foundation for support.

M-AM-E2

ROLE OF K^+ CHANNELS IN REGULATING CALCIUM SIGNALING IN LEUKEMIC T LYMPHOCYTES. Richard S. Lewis[1], Stephan Grissmer[2], and Michael D. Cahalan[2] (Intro. by D.A. Baylor). [1]Department of Molecular & Cellular Physiology, Stanford University Medical School, Stanford, CA 94305, and [2]Department of Physiology & Biophysics, UC Irvine, Irvine, CA 92717.

Mitogenic stimulation of human T lymphocytes evokes intracellular $[Ca^{2+}]$ oscillations that depend on mitogen-regulated Ca^{2+} channels in the plasma membrane. Although the gating of these Ca^{2+} channels is voltage-independent, Ca^{2+} influx is governed by the electrical driving force, which is thought to be established primarily by K^+ conductance. We have used fluorescence video-imaging techniques and high-affinity toxins to study the role of K^+ channels in modulating mitogen-induced Ca^{2+} signaling. Human leukemic T cells (Jurkat E6-1) were loaded with fura-2 (3 μM fura-2/AM for 30 min at 37°C) and bathed in Ringer solution containing 100 nM bis-oxonol [diBAC$_4$(3)]. $[Ca^{2+}]_i$ changes were assessed by exciting fura-2 selectively at 345 or 375 nm, while membrane potential was monitored by exciting bis-oxonol at 490 nm; emission from both dyes was collected at λ >510 nm. Stimulation with 10 μg/ml phytohemagglutinin, a potent T-cell mitogen, elicited parallel oscillations of $[Ca^{2+}]_i$ and membrane potential with a period of 100-200 s. Jurkat cells express primarily two types of K^+ channels that could contribute to this response: voltage-gated K^+ channels that are blocked by charybdotoxin (CTX; K_i=1 nM), and Ca^{2+}-activated K^+ channels sensitive to apamin (K_i<1 nM). CTX (40 nM) or apamin (10 nM) alone had little or no effect on $[Ca^{2+}]_i$. In contrast, simultaneous addition of the two toxins caused membrane depolarization and inhibited $[Ca^{2+}]_i$ oscillations in ~70% of cells undergoing oscillations at the time of treatment. These results suggest that K^+ channels modulate Ca^{2+} signaling in activated T cells by influencing the membrane potential and thus regulating the driving force for Ca^{2+} entry. The lack of effect of either blocker alone indicates that voltage-gated and Ca^{2+}-activated K^+ channels are each capable of fulfilling this function.

M-AM-E3

AGONIST-SPECIFIC MODES OF CALCIUM MOBILIZATION IN CULTURED ENDOTHELIUM William H. Weintraub and Terry E. Machen. Department of Molecular and Cell Biology. University of California at Berkeley, CA 94720.

Regulation of cytosolic free calcium (Cai) by the vasoactive agonists thrombin, bradykinin (BK), and ATP was studied by digital image processing of fura-2 loaded calf pulmonary artery endothelial cells. Maximal doses of these agonists caused Cai to increase from 52 nM to 248, 541, and 643 nM for thrombin, BK, and ATP respectively. Repeated stimulation with thrombin and BK resulted in desensitization of the Cai response. Cells responded heterogeneously to thrombin and BK, and temporal characteristics of the Cai response were conserved upon restimulation even though the amplitude of the ΔCai was reduced. A second addition of agonist after an initial exposure >2.5 minutes resulted in a Cai-transient that was 33%, 17%, and 86% of the initial transient for thrombin, BK, and ATP respectively. Desensitization of the Cai response to thrombin and BK was agonist-specific, and ATP evoked large increases in Cai in both Ca-containing and Ca-free media after the other agonists had lost their ability to do so. These data suggest that endothelial cells can discriminate between different agonists that increase Cai by responding in desensitizing or non-desensitizing modes, and that homologous desensitization to thrombin and BK is controlled at a step prior to activation of phospholipase C.

M-AM-E4

SEPARATE PATHWAYS FOR CARBACHOL-STIMULATED CA INFLUX AND INTRACELLULAR STORE FILLING IN GASTRIC CELLS. P. A. Negulescu and T.E. Machen, Department of Molecular and Cell Biology, University of California at Berkeley, Berkeley CA 94720.

Cholinergic stimulation of gastric cells releases Ca from intracellular stores and stimulates increased Ca influx from the extracellular space. When the stimulus is removed, Ca influx through the cholinergic-stimulated pathway decreases but the internal Ca store refills by taking up Ca across the plasma membrane, possibly *via* a pathway distinct from that regulated by carbachol (carb). We investigated the mechanisms responsible for Ca entry stimulated by carb (CE) and Ca entry due to internal store refilling (RE) using digital image processing of fura-2 fluorescence from intact gastric glands. CE was determined as the steady-state cytosolic Ca (Cai) achieved during treatment with 100μM carb. RE was assessed by measuring the ability of carb to raise Cai in Ca-free solutions. It was possible to distinguish between CE and RE based on CE's increased sensitivity to both LaCL3 and external pH (pHo). CE was blocked at 30μM La while more than 500μM La was required to block RE. CE was inhibited at pHo 6.5 while RE was unaffected at pHo as low as 6.0. Intracellular pH (pHi) changes had no apparent effects on Cai metabolism. CE was unaffected by NH4-induced acidification of pHi. Ca pumping across the plasma membrane was also pHi-independent between 6.5 and 8.0 as determined by the rates at which cells extruded Ca when stimulated in solutions containing 30μM La. We conclude that CE and RE are mediated by separate influx pathways.

M-AM-E5

INTRACELLULAR Ca^{2+} OSCILLATION AND ELECTRICAL BURSTING BY THE MEMBRANE ION CHANNELS AND CELLULAR ENDOPLASMIC RETICULUM IN INSULIN SECRETING PANCREATIC β-CELLS.

Teresa Ree Chay, Department of Biological Sciences, University of Pittsburgh, Pittsburgh, PA 15260

The electrical activity of pancreatic β-cells is determined by a net flow of currents through a number of different types of ion channels across the plasma membrane. The activity of these channels is influenced by the several intracellular events that are triggered by addition of secretagogues. By mathematical modelling, we studied the origin of cyclic changes of intracellular Ca^{2+} concentration ($[Ca^{2+}]_i$) and electrical bursting upon addition of glucose. This model contains two Ca^{2+}-dependent currents: (1) A Ca^{2+} current I_{Ca} that is inactivated slowly by depolarization and by an increase in $[Ca^{2+}]_i$ and (2) a K^+ current $I_{K(Ca,V)}$ that is activated by both voltage and Ca^{2+}. In addition to these currents, the model contains two Ca^{2+}-insensitive currents: (1) A voltage-activated delayed rectifying K^+ current I_K which participates in repolarization of spikes and (2) an inward rectifying ATP-sensitive voltage-independent K^+ current $I_{K,ATP}$ which controls the plateau fractions. Important features of the model are: (1) Glucose inhibits $I_{K,ATP}$ by increasing [ATP]; (2) an inhibition of $I_{K,ATP}$ gives rise to depolarization, which in turn activates the voltage-dependent Ca^{2+} channels; (3) there is a rapid increase in $[Ca^{2+}]_i$ due to the influx of Ca^{2+} ions from the extracellular medium through the Ca^{2+} channels; (4) this increase of $[Ca^{2+}]_i$ triggers a release of Ca^{2+} ions from endoplasmic reticulum (ER) via the Ca^{2+}-induced Ca^{2+} release mechanism; and (5) the release of Ca^{2+} results in a biphasic increase in $[Ca^{2+}]_i$. The model predicts that the electrical spikes on the top of plateaus are due to rapid fluctuations in localized Ca^{2+} ions underneath the plasma membrane. The termination of the plateau is caused by inactivation of I_{Ca} via the release of Ca^{2+} ions by ER and depolarization during the plateau. In addition, the model accommodates the roles of GTP-binding proteins, phosphorylation of I_{Ca}, agonists and antagonists of protein kinase C, and inositol 1,4,5-trisphosphate in the $[Ca^{2+}]_i$ oscillation and electrical activity.

M-AM-E6

CELL-CELL CHANNEL FORMATION INVOLVES DISULFIDE EXCHANGE.

G. Dahl, E. Levine, C. Rabadan-Diehl and R. Werner. Depts. of Physiology and of Biochemisty, University of Miami, Miami, Florida 33101.

The oocyte cell-cell channel assay was used to identify amino acids involved in the process of cell-cell channel formation. The expression of the rat liver gap junction protein connexin32 in single oocytes results in the accumulation of a pool of channel precursors. Upon pairing of such oocytes, cell-cell channels form rapidly from this pool. The rate of formation of cell-cell channels is affected by thiol-specific reagents and pH. This suggests the involvement of extracellular cytsteine residues in the channel formation process. Two connexin32 mutants were generated by site-directed mutagenesis in which cysteine residues were replaced by serines. Both mutant connexins were unable to form cell-cell channels. Thus these cysteines appear to play a crucial role in the channel formation process.

M-AM-E7

REGULATION OF GAP JUNCTIONS BY Ca^{2+} AND PHORBOL 12-MYRISTATE 13-ACETATE (TPA) IN AN MDCK CELL LINE.

V.M. Berthoud, *M.L.S. Ledbetter, E.L. Hertzberg and J.C. Sáez. Dept. Neuroscience, A. Einstein Coll. of Med., Bronx, NY 10461 and *Dept. of Biology, Coll. of the Holy Cross, Worcester, MA 01610.

MDCK cell lines have been widely used in studies of several components of the junctional complex present in epithelia. Extensive studies on gap junctions in these cells have not, however, been reported. It is now accepted that gap junctions are formed by a family of highly homologous proteins (connexins, Cxs) that show differential expression in different cell types. Rat Cxs 32 and 43 are phosphoproteins. Using specific antibodies directed against rat Cx43, we identified reactivity in MDCK (NBL-2) cells by immunoblotting and immunocytochemistry. In immunoblots of total cell homogenates resolved on 10% SDS-PAGE, three bands were detected; approximately 90% of the immunoreactivity was associated with a 41 kDa protein (the dephospho form of Cx43) and the remainder with a 43 kDa doublet. By immunofluorescence, the reactivity was localized between membrane appositions and in the cytoplasm. The incidence of dye coupling (microinjection of Lucifer yellow) and levels of Cx43 increased during logarithmic growth and decreased at or near confluency. The incidence of dye coupling was reduced from 100% to 0% when cells during logarithmic growth were placed in Ca^{2+}-free medium for at least 3 h; this treatment also caused a drastic reduction in levels of Cx43 with no apparent change in the 43 kDa/41 kDa ratio, rounding up of the cells and disappearance of reactivity at remaining membrane appositions. Addition of 2 mM Ca^{2+} for three hours resulted in recovery of adhesiveness and levels of Cx43 and partial recovery of dye coupling. Treatment with 600 nM TPA for as short as 30 min resulted in reduction of the incidence of dye coupling from 100% to 10%. Contact and immunoreactivity between cells were retained by 0.5 h, somewhat reduced by 1 h and drastically reduced by 3 h after treatment, with an increase in cytoplasmic immunoreactivity. At all time points studied, the amount of the 43 kDa form of Cx43 increased and that of the 41 kDa form decreased. Phosphatase treatment of homogenates of TPA-treated cells indicated, in immunoblots, conversion of the 43 kDa form to the 41 kDa form. These data suggest that the regulation of gap junctions by Ca^{2+}-free medium and TPA are partially independent. The effect of Ca^{2+} on Cx43 levels might be related to Ca^{2+}-dependent cell adhesion if levels of Cx43 are controlled by cell contact. The effects of TPA, instead, showed a different time course and phosphorylation of Cx43 parallel with dye uncoupling that preceded the loss of cell contacts.

M-AM-E8

ALPHA-HELICAL STRUCTURE OF CARDIAC GAP JUNCTION ION CHANNELS REVEALED BY CIRCULAR DICHROISM SPECTROSCOPY

Mark Yeager (Intro. by John A. Tainer)

Dept. of Molecular Biology - Research Institute of Scripps Clinic
Div. of Cardiovascular Diseases - Scripps Clinic; La Jolla, CA 92037

Cardiac gap junctions (CGJ) electrically couple myocardial cells to mediate intercellular action potential propagation. The quaternary structure of CGJ is characterized by a hexameric arrangement of 43kD protein subunits with a central ion channel. The protein subunits can be protease-cleaved from 43kD to a membrane-bound form of ~30kD with release of a soluble ~13kD cytoplasmic peptide(s). Protease-cleaved CGJ retain the hexameric channel motif. Analysis of the 30kD amino acid sequence predicts 4 hydrophobic domains of sufficient length to span the lipid bilayer. The secondary structure of 30kD CGJ was examined using circular dichroism (CD) spectroscopy to assess whether the hydrophobic domains are folded as transmembrane α-helices. Rat ventricular CGJ were isolated by routine cell fractionation techniques exploiting the resistance of CGJ to sarkosyl extraction [Manjunath et al., *J. Membrane Biol. 85*: 159-168 (1985)]. Gel electrophoresis and immunoblotting with site-specific peptide antibodies confirmed that CGJ isolated in the absence of PMSF were quantitatively cleaved by an endogenous protease to 30kD. To minimize light scattering, CGJ were sonicated and then centrifuged to remove residual aggregates. CD spectra of CGJ (~1-mg/ml protein) and dialysis buffer (1-mM bicarbonate; pH 8) were recorded at room temperature from 300-185 nm using an AVIV spectropolarimeter with a 1-mm pathlength. Multiple sample spectra and buffer spectra were separately averaged and smoothed, and then subtracted. The corrected sample spectra displayed considerable similarity to the spectra for polypeptides with known α-helical secondary structure. The α-helical content of the 30kD protein was estimated by a linear-least-squares fit of the corrected, experimental spectra to basis spectra for polypeptides with known secondary structures. Examination of the amino acid sequence of 30kD CGJ showed that the experimental α-helical content (40+/-10%) was sufficient to account for α-helical folding of all 4 hydrophobic domains. A working model is that the transmembrane portion of cardiac gap junction ion channels is formed by a hexamer of protein subunits each with a transmembrane 4 α-helical bundle.

Supported by NIH Clinical Investigator Award HLO2129 and AHA National Center Grant-in-Aid 881153.